Site-Specific Difference 2D-IR Spectroscopy of Bacteriorhodopsin

Esben Ravn Andresen and Peter Hamm*

Physikalisch-Chemisches Institut, Universität Zürich, Winterthurerstrasse 190, 8057 Zürich, Switzerland

Received: November 26, 2008; Revised Manuscript Received: January 16, 2009

We demonstrate the extension of the principle of difference Fourier transform infrared (FTIR) spectroscopy to difference 2D-IR spectroscopy. To this end, we measure difference 2D-IR spectra of the protein bacteriorhodopsin in its early J- and K-intermediates. By comparing with the static 2D-IR spectrum of the protonated Schiff base of all-*trans* retinal, we demonstrate that the 2D-IR spectrum of the all-*trans* retinal chromophore in bacteriorhodopsin can be measured with the background from the remainder of the protein completely suppressed. We discuss several models to interpret the detailed line shape of the difference 2D-IR spectrum.

Introduction

Because of the sheer size of a protein, and hence the large number of bonds, it is difficult to obtain any site-specific information from static infrared spectra, whether they are linear or nonlinear. Peaks from individual bonds are usually buried in the background from the rest of the protein. Some nonlinear IR measurements have already been done on proteins, mainly utilizing the amide I band;[1−7] however, these measurements are not site-specific, because the amide I band is a broad, delocalized band whose contributions are distributed over large regions of the protein. Other works utilize cofactors with large IR cross sections in noncongested spectral regions such as CO,[8−14] NO,[15] or CN.[16] This approach is limited to proteins which bind these cofactors, particularly heme proteins.

A more general way of addressing potentially single bonds at a predetermined site in a protein is to incorporate amino acids with side groups with absorptions in noncongested spectral regions, for example S−H groups.[17] Other potential candidates would be non-natural amino acids with groups such as nitrile groups[18,19] or C−D groups.[20−23] Site-specific isotope labeling of the amide I band is yet another potential option, which has been demonstrated for peptides[24,25] and even attempted for the small protein cytochrome *c*,[26] but owing to the typically small isotopic shifts of bands typically employed for 2D-IR spectroscopy, especially the C═O band, the isotope-shifted bands might overlap with bands from other amino acid side chains, e.g., from arganine. Hence, spectroscopic information often has to be derived from the difference spectrum between the artificial and the wild-type protein[27−30] which requires the two spectra to be measured under exactly the same conditions. It would be of considerable interest if a method could be devised for nonlinear infrared spectroscopy that would provide site-specific spectroscopic information from a protein without requiring alterations of the wild-type protein.

In switchable proteins, i.e., molecules whose conformation can be altered electrochemically, photochemically, or by temperature jumps, site-specific information may be obtained by forming a difference spectrum between the switched and nonswitched molecules, thereby singling out the modes that change upon switching[31−34] The concept of photoswitching has been used extensively in various difference FTIR studies particularly of bR,[31] as well as other photoactive proteins.[35−37] The advantage of this approach is that the two spectra from which the difference spectrum is to be formed can be measured quasi-simultaneously, typically within a few milliseconds, which to a large extent cancels out drifts in the experimental setup. Difference Fourier transform infrared (FTIR) is a linear spectroscopy, but the concept of difference spectroscopy should be extendable to nonlinear spectroscopy, i.e., in the context of the present paper, 2D-IR spectroscopy. As in difference FTIR spectroscopy, difference 2D-IR spectroscopy should allow one to measure the 2D-IR spectrum of bands that change upon switching. A further benefit of photoswitchable proteins is that spectra can be measured in a time-resolved manner, thus allowing studies of nonequilibrium dynamics of various protein mechanisms on the femtosecond time scale.

The motivation for extending one-dimensional difference spectroscopy into two dimensions lies in the additional information that two-dimensional spectra can potentially yield, i.e., homogeneous and inhomogenous broadening parameters, ultrafast spectral diffusion dynamics, as well as the connectivity between certain molecular groups. 2D-IR spectroscopy is the optical analogue of two-dimensional NMR spectroscopy (2D-NMR);[38] whereas 2D-NMR spectroscopy measures the couplings between nuclear spins, 2D-IR spectroscopy measures the coupling between molecular vibrations and can be employed on a much faster time regime, down to ∼1 ps. When two vibrations are coupled, cross-peaks show up in a 2D-IR spectrum. From the connectivity between various molecular groups, one can in principle infer the 3D structure of the molecule. To date, 2D-IR spectroscopy has already proven to be useful in the study of fast conformational dynamics of relatively small peptides.[2,3,25,39−42] The next logical step would be to study larger systems, i.e., proteins, however, still maintaining site-selectivity. In the present paper, we introduce the technique of difference 2D-IR spectroscopy, choosing a well-studied system, bacteriorhodopsin (bR), as a demonstration example.

bR[43] is a 26 kDa transmembrane protein composed of 249 amino acids found in the bacterium *Halobacterium salinarium* where it functions as a light-activated proton pump that establishes a proton gradient across the cell membrane for ATP production. bR exists in two conformations, bR_{548} and bR_{568},

* To whom correspondence should be addressed. E-mail: phamm@pci.uzh.ch.

10.1021/jp810397u CCC: $40.75
Published on Web 04/09/2009

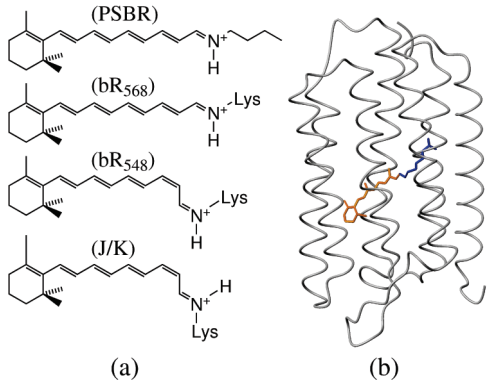

Figure 1. (a) Conformation of retinal in the four different molecules studied in this paper. (b) Structure of bR_{568} with the all-*trans* retinal in orange and Lys216 in blue.

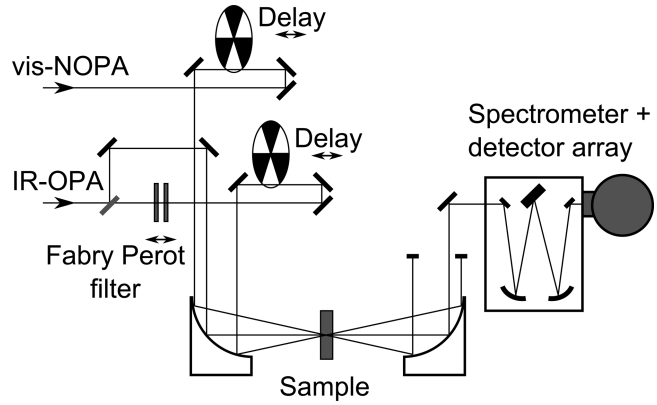

Figure 2. The experimental setup for difference 2D-IR spectroscopy.

only the latter of which undergoes the photocycle. In the dark, these conformations are present in roughly equal amounts, leading to a visible absorption maximum of 555 nm. This is referred to as the "dark-adapted" state of bR. Under illumination with yellow light, bR exists in the "light-adapted" state, in which only bR_{568} is present.[44,45] The initial few hundred femtoseconds of the photocycle involves the chromophore, retinal, switching from the all-*trans* state to the energetically higher-lying 13-*cis* state,[46,47] which stores energy for the rest of the thermally activated proton-pumping cycle. The series of spectroscopically distinct intermediates in the bR photocycle are termed J, K, L, M, N, and O, of which the J- and K-intermediates are formed on the picosecond time scale, and the rest on the microsecond time scale or slower. Sketches of bR and the retinal conformation in bR_{568}, bR_{548}, J, and K are given in Figure 1. BR is an extremely well-studied system and is regarded as a model system for the proton-pumping cycle. Despite this fact, an interest in bR itself persists, and research on it continues.[43,48−50] In particular, with the advances in difference FTIR in recent years, infrared studies have become able to study moieties with ever-smaller extinction coefficients; the latest development has been the study of individual water molecules inside the protein.[50−60] The fact that the initial isomerization of all-*trans* retinal in bR drives the structural changes in the protein that constitute the photocycle or, conversely, that the retinal in bR isomerizes significantly different from free retinal indicates that there are important interactions between the retinal chromophore and the protein itself. However, these interactions are difficult to quantify. Difference 2D-IR is a tool that has the potential to elucidate this interaction due to its sensitivity to changes in the anharmonic coupling not only between modes within the chromophore but also between a mode in the chromophore and a mode in the protein.

The aim of this paper is to demonstrate the feasibility of difference 2D-IR spectroscopy by using the technique to selectively measure the 2D-IR spectrum of the chromophore of bR inside the protein by completely separating it from the protein 2D-IR spectrum. From the perspective of the experimental setup, difference 2D-IR spectroscopy is the same as transient 2D-IR spectroscopy, which has been introduced recently.[7,10,61−69] The distinguishing factor between the two is that, whereas in transient 2D-IR spectroscopy, the purpose is time-resolved studies of molecules having well-characterized vibrational spectra, difference 2D-IR is motivated by the desire to single out individual modes from congested spectra in a not nessecarily time-resolved manner. From our results, we will assess the feasibility of extending the technique to other problems.

Materials and Methods

Difference 2D-IR Spectroscopy. Figure 2 shows a sketch of the experimental setup, the details of which have been described previously.[61] In brief, the light source was a regeneratively amplified Ti:sapphire laser operating at 790 nm with a repetition rate of 1 kHz. An optical parametric amplifier (OPA) delivered stable and tunable mid-infrared pulses of approximately 1.5 μJ pulse energy and pulse duration approximately 100 fs fwhm.[70] The mid-infrared pulses were divided into a strong IR-pump pulse and a weak IR-probe pulse, which were spatially overlapped in the sample in a pump−probe geometry with the IR-probe delayed 1 ps with respect to the IR-pump. The IR-pump pulse was spectrally filtered down to $\sim$15 cm^{-1} by a Fabry−Perot etalon. The 2D-IR spectra were obtained by measuring IR-pump-IR-probe spectra for different IR-pump frequencies and composing a two-dimensional intensity plot versus IR-pump ν_{pump} and ν_{probe} IR-probe frequency.

To initiate the photoreaction in the difference spectroscopy, a noncollinear optical parametric amplifier (NOPA) delivered visible light pulses at $\approx$570 nm with duration of approximately 100 fs fwhm and pulse energies of few microjoules. The vis-pump beam was chopped at 500 Hz, and the IR-pump beam, at 250 Hz. All of the measured 2D-IR and difference 2D-IR spectra were normalized to the IR-pump intensity along the ν_{pump}-axis. The polarizations of all pulses were parallel.

Sample Cell. The 2D-IR spectra of light- and dark-adapted bR were measured on a static sample cell consisting of few microliter sample between two CaF_2 windows separated by a 25 μm spacer. For the 2D-IR spectra of all-*trans* PSBR and the difference 2D-IR spectra of bR, the sample solution was circulated by a peristaltic pump in a closed circle through a flow cell between two CaF_2 windows separated by a 25 μm spacer with a 1-mm-wide flow channel. The flow cell, specifically designed to handle small sample volumes,[71] allowed us to employ volumes down to 300 μL.

Preparation of bR. bR purple membrane patches (PM) were prepared according to standard procedures[72] and provided by Martin Engelhard, Max-Planck-Institute for Molecular Physiology. Difference FTIR experiments on bR are typically performed in films with controlled hydration,[52] in order to maximize protein absorption relative to water absorption. This approach, however, is not feasible for difference 2D-IR measurements, for which rapid sample exchange between laser shots is necessary, and for which extremely low scattering of the IR light is crucial. Hence, the protein needs to be in solution and needs to be quickly circulated through a flow cell. This eventually sets a limit for the viscosity of the protein solution, and hence the

concentration. To reduce the viscosity as much as possible, the size of the PM patches was reduced by sonicating the sample in a Branson cell disruptor and subsequently centrifuging it at 10 000 rpm for 12 min, keeping only the supernatant in the further course of the experiments. Water was removed from the protein by evaporation under vacuum, and the protein was resuspended in D_2O (99.8% d-). Phosphate buffer was added to 15 mM and NaCl to 30 mM. The final concentration of bR was ≈1 mM, the optical density in the visible was ≈0.15, and the optical density in the infrared region from 1490 to 1665 cm^{-1} (the spectral region, in which we did the measurements) was 0.25 to 0.5. After preparation, the function of bR was confirmed by observing that the protein underwent light- and dark-adaption, which can be deduced from the visible spectrum: After storage in the dark for a few hours, the absorption maximum was at 555 nm, which indicates that bR is dark-adapted; after illumination with yellow light, the absorption maximum was at 568 nm, which indicates that bR is light-adapted.[44,45]

Preparation of the Schiff Base of All-*trans* Retinal. As a reference sample, we also measured the retinal chromophore outside a protein environment in the form of all-*trans* retinylidene *n*-butylamine, i.e., the protonated Schiff base of all-*trans* retinal (all-*trans* PSBR). To that end, 17 mM all-*trans* retinal was condensed with a 10-fold excess of *n*-butylamine in dry ether.[73] All-*trans* retinal and *n*-butylamine were purchased from Sigma-Aldrich. Excess amine and ether was removed under reduced pressure to yield a powder consisting of the Schiff base. The mixture was kept in the dark and under nitrogen during the preparation. For the measurements, the Schiff base was suspended in dry ethanol in a concentration of 10 mM. Protonation was performed with 150 mM HCl in dry ethanol, added to the Schiff base solution up to a 3-fold excess of HCl. In the measurements, a volume of 50 mL of the PSBR solution was circulated under nitrogen and in the dark. A sketch of PSBR can be seen in Figure 1.

Results

2D-IR Spectroscopy of All-*trans* PSBR. As a reference molecule, we start with the spectroscopy of the isolated chomophore in solution (all-*trans* PSBR, Figure 3). The absorption (1D-IR) spectrum (Figure 3a) is dominated by two strong peaks. The peak at 1558 cm^{-1} has been assigned to an ethylenic mode of the retinal backbone[74] which is much stronger than the other three ethylenic modes that are expected from the backbone of four C═C bonds found in retinal. The peak at 1657 cm^{-1} has been assigned to a band arising from mostly the C═N vibration.[74]

The corresponding 2D-IR spectrum is presented in Figure 3b. Two diagonal peaks are clearly visible at 1558 cm^{-1} (ethylenic stretch, "C1") and 1657 cm^{-1} (C═N stretch, "C2") at the positions predicted by the absorption spectrum (Figure 3a). Also visible are the two cross-peaks ("C21" and "C12") connecting these two bands, reporting on the coupling between them. The essential features are most clearly seen in the horizontal cuts of the 2D-IR spectrum in Figure 3c (ν_{pump} = 1657 cm^{-1}) and d (ν_{pump} = 1558 cm^{-1}). We expect that the features of Figure 3 will be reproduced in the 2D-IR spectrum all-*trans* PSBR situated in the protein environment, albeit at slightly shifted frequencies due to the different chemical surrounding.

Conventional 2D-IR Spectroscopy of bR. In a next step, we present static 2D-IR spectra of dark- and light-adapted bR as the initial attempt at identifying the chromophore bands inside the protein. In the dark-adapted state, bR adopts two different confirmations in roughly equal amounts, bR_{568} and bR_{548},[44] with the subscripts denoting the visible absorption maximum. BR_{568} undergoes the proton-pumping photocycle and contains the *all-trans*-15-*anti*-chromophore, while bR_{548} does not pump protons and contains a 13-*cis*-15-*syn*-chromophore. The frequencies of the two strong bands of the chromophore inside the protein, corresponding to the same ones as observed in solution (Figure 3a), are known from resonance-Raman studies. They are found at 1528 cm^{-1} (ethylenic stretch) and 1624 cm^{-1} (C═N stretch) in bR_{568} (in D_2O)[75] and shift to 1534 and 1618 cm^{-1} in bR_{548}.[44]

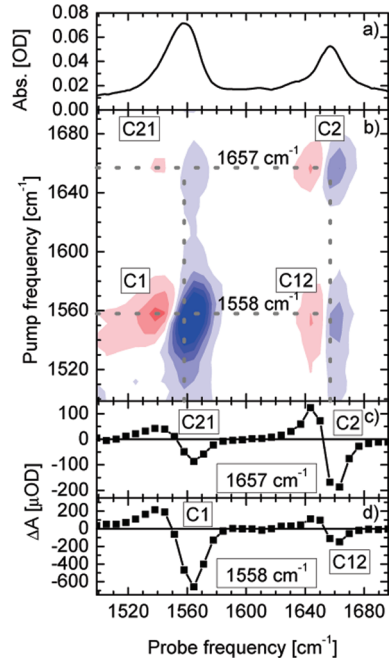

Figure 3. (a) Absorption (1D-IR) spectrum of PSBR with the solvent background subtracted. (b) 2D-IR spectrum of all-*trans* PSBR. (c and d) horizontal cuts at ν_{pump} = 1657 cm^{-1} and ν_{pump} = 1558 cm^{-1}, repsectively. The labels C1, C2, C12, and C21 refer to signals discussed in the text. Blue colors refer to negative signals (bleach and stimulated emission), and red colors, to positive signals (excited-state absorption).

Figure 4a,b shows the absorption spectra of dark- and light-adapted bR. As expected, these spectra are dominated by the strong, broad amide I and II bands at 1650 and 1550 cm^{-1}, respectively. Figure 4c,d shows the corresponding 2D-IR spectra, which appear similar to each other in all major features. As in the absorption spectra, the dominant features are the diagonal peak of the amide I band ("AI"), the diagonal peak from the amide II band ("AII"), and the cross-peaks connecting them ("AI-II" and "AII-I").

In the lower-right off-diagonal region, an additional cross-peak "C12" is clearly visible, which, based on its frequency, we assign to a cross-peak between the two dominant chromophore bands. The corresponding diagonal peaks "C1" and "C2", as well as the upper-left cross-peak "C21", are less apparent, since they are superimposed on the much stronger amide I and II signals. Nevertheless, from a comparison of the two spectra from dark- and light-adapted bR, we can in fact identify some of these signals. To this end, we compare horizontal cuts of the 2D-IR spectra, Figure 4e−h. Examining the line shape at "C1" in Figure 4g and h, one observes a clear difference from the dark- to the light-adapted case. Cross-peak "C21" is not visible in dark-adapted bR (Figure 4e), possibly due to overlap with other cross-peaks such as "AI-II", but it

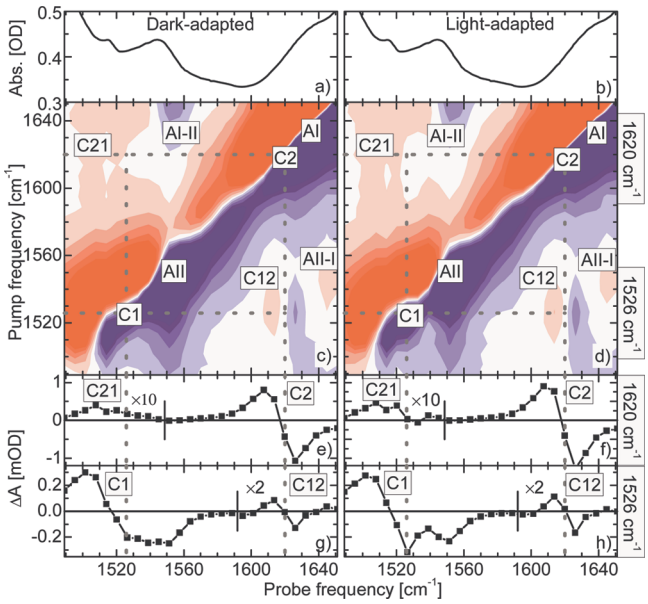

Figure 4. (a, b) Absorption (1D-IR) spectra of dark- and light-adapted bR in D_2O. (c, d) 2D-IR spectra of dark- and light-adapted bR. Horizontal cuts at (e, f) $\nu_{pump} = 1620$ cm^{-1} and at (g, h) $\nu_{pump} = 1526$ cm^{-1}, respectively. Blue colors refer to negative signals (bleach and stimulated emission), and red colors, to positive signals (excited-state absorption). The noise in parts e−h was less than 0.01 mOD. Important spectral features are labeled and discussed in the text.

shows up in the light-adapted case (Figure 4f). On the other hand, the spectral region where "C2" is expected (Figure 4e and f) is dominated by the amide I band, and no distinct feature that could be assigned to the C═N diagonal peak is observed. We thus do see signatures of the chromophore in the static 2D-IR spectra. This might seem somewhat surprising, since one might expect that the amide I and amide II diagonal and cross-peaks are much stronger compared to the chromophore bands due to the sheer number of modes that contribute. One explanation is that the amide modes of the protein backbone delocalize due to excitonic coupling, which leads to a decrease in their anharmonicity and, hence, in their 2D-IR intensity.[76] In addition, 2D-IR spectroscopy amplifies in a relative sense the contribution of strong absorbers, since 2D-IR spectroscopy scales quadratically with the extinction coefficient.

Although care was taken to record the dark- and light-adapted spectra under similar conditions, and in succession of one another, slight drifts in instrumental parameters prohibit taking the difference between the two spectra and thereby completely suppress the protein background. Thus, difference 2D-IR spectra should be calculated from spectra that are measured quasi-simultaneously, by which is meant that the difference spectrum is formed from measurements of pumped and unpumped sample at consecutive laser shots. This is a well-known fact from difference FTIR spectroscopy.[77]

Difference 2D-IR Spectroscopy of BR. With these preliminary results in mind, we now turn to difference 2D-IR spectroscopy of bR (Figure 5). Three different vis-pump-IR-probe delay times were chosen, while the IR-pump-IR-probe delay was held fixed at 1.0 ps in all three cases (dictated by the typical vibrational dephasing time in the condensed phase): At a vis-pump-IR-probe delay of 1.3 ps, the IR-pump follows 0.3 ps after the vis-pump; hence, this delay scheme represents the shortest possible delay after photoactivation, which can be probed without compromising the time ordering of the pulses. This delay scheme should then give the largest bleach signal. At a vis-pump-IR-probe delay of 2.0 ps, the IR-pump-IR-probe sequence falls in the time interval 1.0−2.0 ps, or 2−4 time constants for the formation of the J-intermediate (time constant, 0.5 ps)[78] after photoactivation; hence, mostly the intermediate is measured. Finally, at a vis-pump-IR-probe delay of 21 ps, we expect that the K-intermediate is fully formed (time constant of formation, 3 ps).[78]

The difference 1D-IR spectra show a bleach of the two dominant ethylenic and C═N stretch vibrations of the chromophore (Figure 5a−c), together with a red-shifted product contribution from the ethylenic band.[49] The bleach partially recovers as a function of delay time, reflecting cooling of the system. The corresponding difference 2D-IR spectra at the same vis-pump-IR-probe delay times are shown in Figure 5d−f as contour plots as well as horizontal cuts at four different pump frequencies (Figure 5g−r). One immediately observes the absence of the large contributions from the protein bands, i.e., the dominant features in the static 2D-IR spectrum (Figure 4c,d), "AI" and "AII", which have been completely canceled out by forming the difference spectrum. The difference 2D-IR spectrum has singled out the four peaks "C1", "C2", "C12", and "C21". On the basis of their frequency, these four peaks are assigned to the ethylenic ("C1") and the C═N ("C2") stretch vibration of the chromophore, and to a cross-peak connecting them. Peaks "C2", "C21", and "C12" have inverted signs, compared to the static 2D-IR spectrum of all-*trans* PSBR, Figure 3 (the signs are color-coded in red and blue in Figure 5d−f, see also cuts in Figure 5g−r). Since these spectra originate from a difference between visible-pumped minus unpumped sample, the inverted sign indicates that these signals reflect the bleach of the ground-state bR_{568} contribution. The transient photoproducts have negligible intensity for C═N vibration (see Figure 5a−c), and consequently, their contribution to peaks "C2", "C21", and "C12" is minor as well. These three peaks are strongest at a vis-pump-IR-probe delay of 1.3 ps and partially recover with increasing delay times, just like they do in the difference 1D-IR spectra (Figure 5a−c). The 2D line shape of the diagonal peak "C1", on the other hand, is more complex and will be discussed in the next paragraph.

Line Shape Modeling. From the difference 1D-IR spectra of bR, Figure 5a−c, we see that band "C1" red-shifts in all transient intermediates. As a first step, we consider a simple model that would take this red-shift into account (Figure 6). The reactant 2D-IR spectrum Figure 6a displays a diagonal signal for each band, "C1" and "C2". Each signal is composed of a positive and a negative peak separated by the anharmonicity. The coupling between the two bands leads to the appearance of cross-peaks "12" and "21" that are also composed of a positive and a negative peak. For the transient photoproduct state, we assume that peak "C1" is red-shifted whereas peak "C2" bleaches, Figure 6b. This qualitatively reproduces the difference 1D-IR spectrum, and also peaks "C2", "C12", and "C21" in the difference 2D-IR spectrum agree well with experiment. However, for peak "C1", the model 2D-IR spectrum is in contradiction with the measurement, as it gives a 2D-IR line shape that seems to be inverted compared to the experimental results. In particular, the strongest band in the center of peak "C1" is negative (blue) in the model spectrum, whereas it is positive (red) in the early experimental spectra (Figure 5a,b).

The remedy lies in the fact that more than one normal mode contributes to the complex 2D-IR response in the "C1" spectral region (Figure 7). In fact, if we add one more product band for the K-intermediate at 1535 cm^{-1}, which turns out to be relatively weak and narrow and is responsible for the small dip in the bleach of the difference 1D-IR spectrum (see arrow in Figure

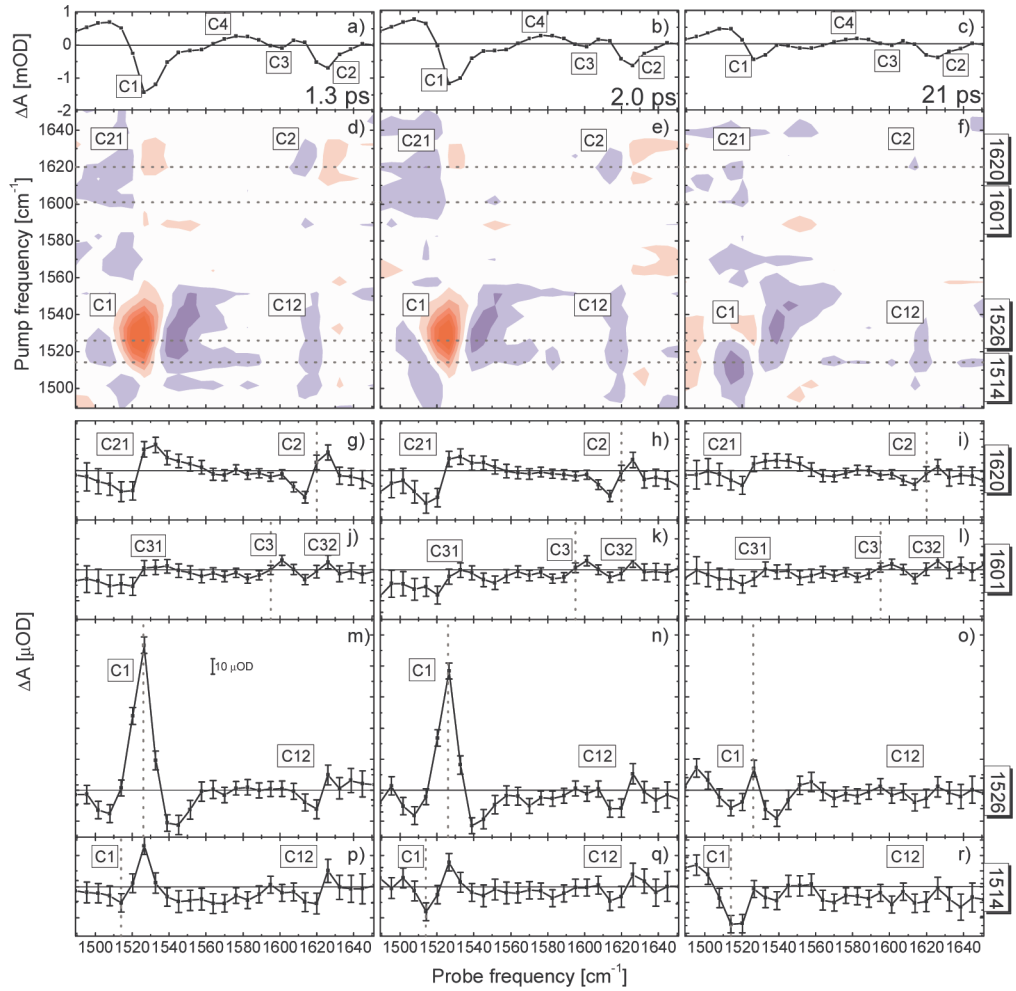

Figure 5. Difference spectra of bR at (first column) 1.3 ps, (second column) 2.0 ps, and (third column) 21 ps. (a−c) Difference 1D-IR spectra. (d−f) Difference 2D-IR spectra. Horizontal cuts at (g−i) $\nu_{pump} = 1620$ cm^{-1}, at (j−l) $\nu_{pump} = 1601$ cm^{-1}, at (m−o) $\nu_{pump} = 1526$ cm^{-1}, and at (p−r) $\nu_{pump} = 1514$ cm^{-1}. The 2D-IR spectra (d−f) have been 2D-smoothed, while the other figures have not. The difference 2D-IR spectra were measured in two parts, namely, $\nu_{pump} = 1489.2-1557.6$ cm^{-1} and $\nu_{pump} = 1557.6-1651.0$ cm^{-1}. Blue colors refer to negative signals, and red colors, to positive signals. The error bars denote ±1 standard error. Important spectral features are labeled and discussed in the text.

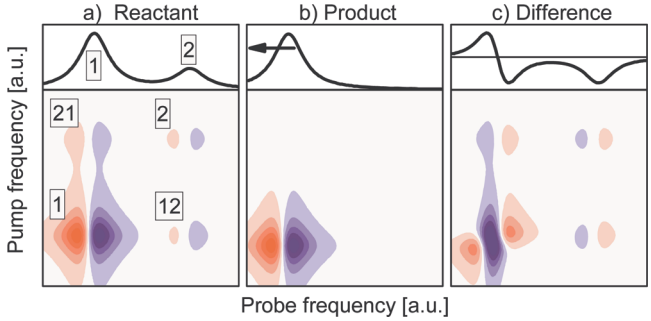

Figure 6. Model 1D-IR and 2D-IR spectra for (a) a reactant state with two coupled bands and (b) a transient photoproduct state where band "C1" is red-shifted and band "C2" is bleached. (c) Corresponding difference IR and difference 2D-IR spectra. Blue colors refer to negative signals, and red colors, to positive signals.

7g), the partial cancelation effects in the 2D-IR line shape become sufficiently complex to allow reproducing the experimental difference 1D-IR and 2D-IR spectra essentially quantitatively (compare cuts in Figure 7i−l). The parameters obtained from this fit are summarized in Table 1. The 1535 cm^{-1} band of this model could be due to the strengthening of the 1534 cm^{-1} band of bR_{568} that was calculated in ref 75. In ref 79, a band at 1534 cm^{-1} has in fact been measured for the K-intermediate, which agrees reasonably with the 1535 cm^{-1} band of our model.

We have not attempted to quantitatively fit peak "C1" at delay times 1.3 and 2.0 ps with a similar model, because the product bands at these early delays might be hot bands, thereby complicating matters.[61] It is nevertheless clear that the spectra contain signatures of bR_{568} bleach as well as from very early transient photoproducts. In particular, the blue band at the high-frequency side of peak "C1", which originates from the weak product band at 1535 cm^{-1} (and which is missing in the simpler model of Figure 6), is present in already the earliest delay time spectra.

Other Spectral Features. Besides the strong chromophore bands discussed above, we also observe weaker features in the difference 1D-IR and 2D-IR spectra. In Figure 5j−l, a small diagonal peak originating from the reactant state is visible (peak "C3"), which we attribute to an ethylenic band of the bR_{568} chromophore. This is in agreement with the bleach in Figure 5a−c at ca. 1600 cm^{-1}, and also consistent with ref 75, which found an ethylenic band at about this position. Additional off-diagonal features are peaks "C31" and "C32" (Figure 5j−l), that could be cross-peaks from mode "C3" to the dominating "C1" and "C2" bands. These signals decay as a function of delay time due to the partial recovery of the initial reactant state. Furthermore, a relatively broad positive band at 1580 cm^{-1} is

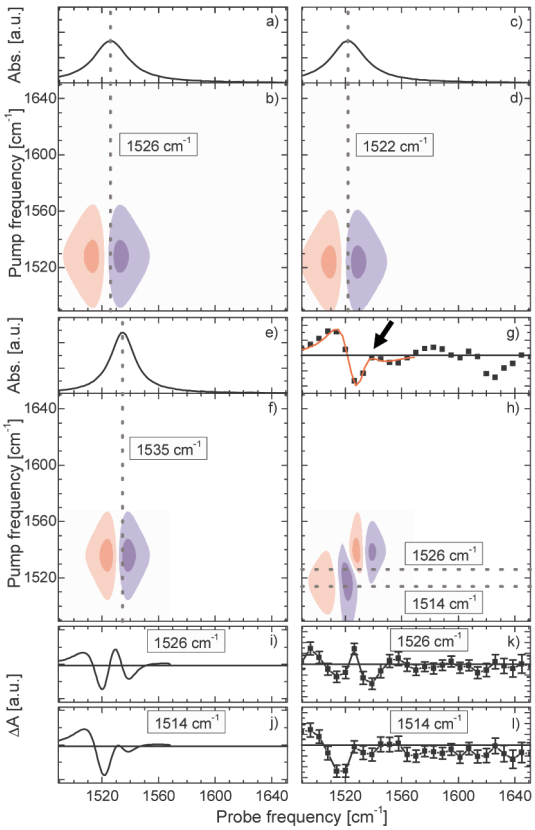

Figure 7. Model spectra with three bands that contribute in the "C1" spectral region: (a, b) one reactant band at 1526 cm^{-1}; (c−f) two product bands at 1522 and 1535 cm^{-1}, respectively. (g, h) The corresponding difference 1D-IR and 2D-IR spectra together with (i, j) horizontal cuts of the simulated difference 2D-IR spectrum at pump frequencies ν_{pump} = 1526 cm^{-1} and ν_{pump} = 1514 cm^{-1}. The latter are compared to the experimental results at a vis-pump-IR-probe delay time of 21 ps in panels g, k, and l. Blue colors in the 2D-IR spectra refer to negative signals, and red colors, to positive signals.

TABLE 1: Parameters Obtained from a Simultaneous Fit of the Difference 1D-IR (Figure 7g) and 2D-IR (Figure 7i−l) Spectra at a Vis-Pump-IR-Probe Delay Time of 21 ps[a]

	homogeneous width (cm^{-1})	anharmonicity (cm^{-1})	relative integrated intensity
reactant 1526 cm^{-1}	30	−7	−1
product 1522 cm^{-1}	30	−7	0.8
product 1535 cm^{-1}	21	−10	0.16

[a] The frequency of the product band at 1522 cm^{-1} was taken from ref 79.

observed in the difference 1D-IR spectra Figure 5a−c (peak "C4"). In the horizontal cuts at ν_{pump} = 1576 cm^{-1} (not shown), we do not observe any clear signature that could correspond to this band. The band position agrees, though, with an ethylenic mode at 1577 cm^{-1}.[75]

Discussion and Conclusion

We have demonstrated that one can extend the very idea of difference FTIR spectroscopy[31,37] to 2D-IR spectroscopy. That is, by quasi-simultaneously measuring a 2D-IR spectrum of a photoactivated and the ground-state bR and subtracting them in the computer, one can completely suppress the inactive protein background and single out 2D-IR signals of individual normal modes from the chromophore (Figure 5). As expected from the static 2D-IR spectrum of all-*trans* PSBR (Figure 3), these two modes are coupled and produce a clear cross-peak in the difference 2D-IR spectrum, indicating that the composition of the normal modes is similar in solution and in the protein environment. The difference 2D-IR response of the chromophore is not as weak as one might expect from the linear absorption spectrum. Partly, this is because 2D-IR intensities scale as the extinction coefficient squared rather than being linear, this amplifying the strong chromophore bands with $\varepsilon \approx 2500$ (Mcm)$^{-1}$ and 1500 (Mcm)$^{-1}$ relative to the amide bands with $\varepsilon \approx 1000$ (Mcm)$^{-1}$.

One possible drawback of difference 2D-IR spectroscopy is the complicated 2D-IR line shapes.[66] Nevertheless, as demonstrated here for peak "C1", a simultaneous fitting of difference 1D-IR and 2D-IR spectra allows one to quite uniquely disentangle the contributions from various modes (Figure 7).

The nature of the earliest J-intermediate is still under debate. While most researchers argue that the J-state is just a vibrationally hot K-state right after an essentially barrierless crossing from the electronically excited state into the isomerized state,[46,47,49,80,81] it has also been speculated that the J-state is a distinct intermediate,[78] possibly involving another electronic state.[82] In previous works,[61] where we have studied the structural response of a short cyclic peptide after the photoisomerization of a azobenzene moiety, we saw in the early 2D-IR difference spectra only the contribution from the initial reactant state, and not from the early photoproduct. We explained this result by the fact that the early photoproduct is vibrationally hot, leading to strong homogeneous broadening. Whenever the homogeneous width is broader than the anharmonic shift between the 0−1 and the 1−2 transition, the partial cancelation of the latter two will render the 2D-IR response of the hot photoproduct very small, and the difference 2D-IR spectrum is dominated by the reactant contribution. In the present case, in contrast, we clearly observe 2D-IR signals also from the very early transient photoproducts, as evidenced by the complex line shape of peak "C1" in Figure 5d. This implies either that the J-state is in fact not just a vibrationally hot K-state or that heating does not lead to homogeneous broadening in this case, possibly due to the very rigid environment inside the protein. In the latter case, difference 2D-IR spectroscopy could in fact be used as a structure sensitive method for even the earliest intermediates.

A requirement for further difference 2D-IR studies of weaker modes would be an improvement of the signal-to-noise ratio. The results of this paper were measured in the pump−probe geometry using a Fabry−Perot etalon to filter the IR-pump pulse. It is expected that an improvement in signal-to-noise ratio could be achieved by measuring in the three-pulse photon echo geometry, in which probe and local-oscillator intensities can be independently set. The extinction coefficient of the C═O mode of 500−1000 (Mcm)$^{-1}$ is similar to that of the bR chromophore C═N ("C2") mode, whose diagonal and cross-peaks we could observe in the difference 2D-IR spectra (albeit, presently, just above the noise level). It is nevertheless expected that the potential improvements outlined above could make it possible to measure 2D-IR spectra of individual C═O modes from the protein backbone in unlabeled proteins by difference 2D-IR spectroscopy. In the case of bR, the protein backbone undergoes significant structural changes in the L-intermediate and later on in the photocycle, as evidenced by transient absorption signals in the amide I and II spectral region that are of similar strength as that of the chromophore.[83] We are currently working in this direction.

In conclusion, we demonstrate that it is possible to obtain site-specific information from 2D-IR spectra of unlabeled,

wild-type proteins by means of difference 2D-IR spectroscopy. In the present study, we use bR as a convenient example to demonstrate the principle of difference 2D-IR, which can be triggered by light. Nevertheless, the concept should be broader. It requires a possibility to quickly switch the state of a protein, ideally between subsequent laser pulses within 1 ms, for instance, electrochemically, as it is also common in difference FTIR spectroscopy,[33] or possibly in a microfluidic flow cell.

Acknowledgment. We are grateful to Martin Engelhard, Max-Planck-Institute for Molecular Physiology, for supplying us with the bR sample and to Friedrich Siebert for many valuable discussions. The work was financially supported by the Danish Natural Science Research Council through a postdoctoral fellowship to E.R.A., as well as by the Swiss National Science Foundation.

References and Notes

(1) Xie, A.; van der Meer, L.; Hoff, W.; Austin, R. H. *Phys. Rev. Lett.* **2000**, *84*, 5435–5438.
(2) Hamm, P.; Lim, M.; Hochstrasser, R. M. *J. Phys. Chem. B* **1998**, *102*, 6123–6138.
(3) Demirdöven, N.; Cheatum, C. M.; Chung, H. S.; Khalil, M.; Knoester, J.; Tokmakoff, A. *J. Am. Chem. Soc.* **2004**, *126*, 7981–7990.
(4) Chung, H. S.; Khalil, M.; Smith, A. W.; Ganim, Z.; Tokmakoff, A. *Proc. Natl. Acad. Sci. U.S.A.* **2005**, *102*, 612–617.
(5) Wang, L.-X.; Meersman, F.; Wu, Y. *J. Mol. Struct.* **2008**, *883*, 79–84.
(6) Ganim, Z.; Chung, H. S.; Smith, A. W.; Deflores, L. P.; Jones, K. C.; Tokmakoff, A. *Acc. Chem. Res.* **2008**, *41*, 432–441.
(7) Chung, H. S.; Ganim, Z.; Jones, K. C.; Tokmakoff, A. *Proc. Natl. Acad. Sci. U.S.A.* **2007**, *104*, 14237–14242.
(8) Lim, M.; Hamm, P.; Hochstrasser, R. M. *Proc. Natl. Acad. Sci. U.S.A.* **1998**, *95*, 15315–15320.
(9) Hamm, P.; Lim, M.; Asplund, M.; Hochstrasser, R. M. *Chem. Phys. Lett.* **1999**, *301*, 167–174.
(10) Ishikawa, H.; Kwak, K.; Chung, J. K.; Kim, S.; Fayer, M. D. *Proc. Natl. Acad. Sci. U.S.A.* **2008**, *105*, 8619–8624.
(11) Ishikawa, H.; Kim, S.; Kwak, K.; Wakasugi, K.; Fayer, M. D. *Proc. Natl. Acad. Sci. U.S.A.* **2007**, *104*, 19309–19314.
(12) Ishikawa, H.; Finkelstein, I. J.; Kim, S.; Kwak, K.; Chung, J.; Wakasugi, K.; Massari, A.; Fayer, M. D. *Proc. Natl. Acad. Sci. U.S.A.* **2007**, *104*, 16116–16121.
(13) Bredenbeck, J.; Helbing, J.; Nienhaus, K.; Nienhaus, G. U.; Hamm, P. *Proc. Natl. Acad. Sci. U.S.A.* **2007**, *104*, 14243–14248.
(14) Finkelstein, I. J.; Zheng, J. R.; Ishikawa, H.; Kim, S.; Kwak, K.; Fayer, M. D. *Phys. Chem. Chem. Phys.* **2007**, *9*, 1533–1549.
(15) Kholodenko, Y.; Gooding, E. A.; Dou, Y.; Ideda-Saito, M.; Hochstrasser, R. M. *Biochemistry* **1999**, *38*, 5918–5924.
(16) Helbing, J.; Bonacina, L.; Pietri, R.; Bredenbeck, J.; Hamm, P.; van Mourik, F.; Chaussard, F.; Gonzalez-Gonzales, A.; Chergui, M.; Ramos-Alvarez, C.; Ruiz, C.; López-Garriga, J. *Biophys. J.* **2004**, *87*, 1881–1890.
(17) Kozinski, M.; Garrett-Roe, S.; Hamm, P. *J. Phys. Chem. B* **2008**, *112*, 7645–7650.
(18) Getahun, Z.; Huang, C. Y.; Wang, T.; DeLeon, B.; DeGrado, W. F.; Gai, F. *J. Am. Chem. Soc.* **2003**, *125*, 405–411.
(19) Lindquist, B. A.; Corcelli, S. A. *J. Phys. Chem. B* **2008**, *112*, 6301–6303.
(20) Sagle, L. B.; Zimmerman, J.; Dawson, P. E.; Romesberg, F. E. *J. Am. Chem. Soc.* **2004**, *126*, 3384–3385.
(21) Kenan, G.; Nydegger, M. W.; Bafndaria, J. N.; Hill, S. E.; Cheatum, C. M. J. *J. Chem. Phys.* **2006**, *125*, 174503.
(22) Kumar, K.; Sinks, L. E.; Wang, J.; Kima, Y. S.; Hochstrasser, R. M. *Chem. Phys. Lett.* **2006**, *432*, 122–127.
(23) Chin, J. K.; Jimenez, R.; Romesberg, F. E. *J. Am. Chem. Soc.* **2001**, *123*, 2426–2427.
(24) Fang, C.; Wang, J.; Kim, Y. S.; Charnley, A. K.; Barber-Armstrong, W.; Smith, A. B., III.; Decatur, S. M.; Hochstrasser, R. M. *J. Phys. Chem. B* **2004**, *108*, 10415–10427.
(25) Mukherjee, P.; Krummel, A. T.; Fulmer, E. C.; Kass, I.; Arkin, I. T.; Zanni, M. T. *J. Chem. Phys.* **2004**, *120*, 10215–10224.
(26) Londergan, C.; Hochstrasser, R. *Abs. Pap. Am. Chem. Soc.* **2005**, *230*, U2930.
(27) Sonar, S.; Lee, C.-P.; Coleman, M.; Patel, N.; Liu, X.; Marti, T.; Khorana, H. G.; RajBhandary, U. L.; Rotschild, K. J. *Nat. Struct. Biol.* **1994**, *1*, 512–517.
(28) Hauser, K.; Engelhard, M.; Friedman, N.; Sheves, M.; Siebert, F. *J. Phys. Chem. A* **2002**, *106*, 3553–3559.
(29) Ludlam, C. F. C.; Sonar, S.; Lee, C.-P.; Coleman, M.; Herzfeld, J.; RajBhandary, U. L.; Rotschild, K. J. *Biochemistry* **1995**, *34*, 2–6.
(30) Sonar, S.; Liu, X.-M.; Lee, C.-P.; Coleman, M.; He, Y.-W.; Pelletier, S.; Herzfeld, J.; RajBhandary, U. L.; Rotschild, K. J. *J. Am. Chem. Soc.* **1995**, *117*, 11614–11616.
(31) Gerwert, K.; Siebert, F. *EMBO J.* **1986**, *5*, 805–811.
(32) Williams, S.; Causgrove, T. P.; Gilmanshin, R.; Fang, K. S.; Callender, R. H.; Woodruff, W. H.; Dyer, R. B. *Biochemistry* **1996**, *35*, 691–697.
(33) Bauscher, M.; Leonhard, M.; Moss, D. A.; Mäntele, W. *Biochim. Biophys. Acta* **1993**, *1183*, 59–71.
(34) Zscherp, C.; Barth, A. *Biochemistry* **2001**, *40*, 1875–1883.
(35) Remy, A.; Gerwert, K. *Nat. Struct. Biol.* **2003**, *10*, 637–644.
(36) Fahmy, K.; Sakmar, T. P.; Siebert, F. *Methods Enzymol.* **2000**, *315*, 178–196.
(37) Kötting, C.; Gerwert, K. *ChemPhysChem* **2005**, *41*, 881–888.
(38) Woutersen, S.; Hamm, P. *J. Phys.: Condens. Matter* **2002**, *14*, R1035−R1062.
(39) Woutersen, S.; Hamm, P. *J. Phys. Chem. B* **2000**, *104*, 11316–11320.
(40) Asplund, M. C.; Zanni, M. T.; Hochstrasser, R. M. *Proc. Natl. Acad. Sci. U.S.A.* **2000**, *97*, 8219–8224.
(41) Maekawa, H.; Toniolo, C.; Moretto, A.; Broxterman, Q. B.; Ge, N. *J. Phys. Chem. B* **2006**, *110*, 5834–5837.
(42) Shim, S.-H.; Strasfeld, D. B.; Ling, Y. L.; Zanni, M. T. *Proc. Natl. Acad. Sci. U.S.A.* **2007**, *104*, 14197–14202.
(43) Lanyi, J. K. *Annu. Rev. Physiol.* **2004**, *66*, 665–688.
(44) Smith, S. O.; Pardoen, J. A.; Lugtenburg, J.; Mathies, R. A. *J. Phys. Chem.* **1987**, *91*, 804–819.
(45) Harbison, G.; Smith, S.; Pardoen, J.; Winkel, C.; Lugtenburg, J.; Herzfeld, J.; Mathies, R.; Griffin, R. *Proc. Natl. Acad. Sci. U.S.A.* **1984**, *81*, 1706–1709.
(46) Dobler, J.; Zinth, W.; Oesterhelt, D. *Chem. Phys. Lett.* **1988**, *144*, 215–220.
(47) Mathies, R.; Cruz, C.; Pollard, W.; Shank, C. *Science* **1988**, *240*, 777–779.
(48) Schenkl, S.; van Mourik, F.; van der Zwan, G.; Hacke, S.; Chergui, M. *Science* **2005**, *309*, 917–920.
(49) Herbst, J.; Heyne, K.; Diller, R. *Science* **2002**, *297*, 822–825.
(50) Garczarek, F.; Gerwert, K. *Nature (London)* **2006**, *439*, 109–112.
(51) Maeda, A.; Morgan, J. E.; Gennis, R. B.; Ebrey, T. G. *Photochem. Photobiol.* **2006**, *82*, 1398–1405.
(52) Lórenz-Fonfría, V. A.; Furutani, Y.; Kandori, H. *Biochemistry* **2008**, *47*, 4071–4081.
(53) Shibata, M.; Kandori, H. *Biochemistry* **2005**, *44*, 7406–7413.
(54) Tanimoto, T.; Furutani, Y.; Kandori, H. *Biochemistry* **2003**, *42*, 2300–2306.
(55) Tanimoto, T.; Shibata, M.; Belenky, M.; Herzfeld, J.; Kandori, H. *Biochemistry* **2004**, *43*, 9439–9447.
(56) Kandori, H.; Shichida, Y. *J. Am. Chem. Soc.* **2000**, *122*, 11745–11756.
(57) Shibata, M.; Tanimoto, T.; Kandori, H. *J. Am. Chem. Soc.* **2003**, *125*, 13312–13313.
(58) Hatanaka, M.; Kandori, H.; Maeda, A. *Biophys. J.* **1997**, *73*, 1001–1006.
(59) Maeda, A.; Tomson, F. L.; Gennis, R. B.; Ebrey, T. G.; Balashov, S. P. *Biochemistry* **1999**, *38*, 8800–8807.
(60) Morgan, J. E.; Vakkasoglu, A. S.; Gennis, R. B.; Maeda, A. *Biochemistry* **2007**, *46*, 2787–2796.
(61) Bredenbeck, J.; Helbing, J.; Behrendt, R.; Renner, C.; Moroder, L.; Wachtveitl, J.; Hamm, P. *J. Phys. Chem. B* **2003**, *107*, 8654–8660.
(62) Bredenbeck, J.; Helbing, J.; Hamm, P. *J. Am. Chem. Soc.* **2004**, *126*, 990–991.
(63) Bredenbeck, J.; Helbing, J.; Hamm, P. *J. Chem. Phys.* **2004**, *121*, 5943–5957.
(64) Kolano, C.; Helbing, J.; Kozinski, M.; Sander, W.; Hamm, P. *Nature (London)* **2006**, *444*, 469–472.
(65) Bredenbeck, J.; Helbing, J.; Kolano, C.; Hamm, P. *ChemPhysChem* **2007**, *8*, 1747–1756.
(66) Cervetto, V.; Hamm, P.; Helbing, J. *J. Phys. Chem. B* **2008**, *112*, 8398–8405.
(67) Hamm, P. *Ultrashort Laser Pulses in Biology and Medicine*; Springer: Berlin, Germany, 2008; pp 7794.
(68) Baiz, C. R.; Nee, M. J.; McCanne, R.; Kubarych, K. J. *Opt. Lett.* **2008**, *33*, 2533–2535.
(69) Chung, H. S.; Khalil, M.; Smith, A. W.; Tokmakoff, A. *Rev. Sci. Instrum.* **2007**, *78*, 063101.
(70) Hamm, P.; Kaindl, R. A.; Stenger, J. *Opt. Lett.* **2000**, *25*, 1798–1800.
(71) Bredenbeck, J.; Hamm, P. *Rev. Sci. Instrum.* **2003**, *74*, 3188–3189.

(72) Oesterhelt, D.; Stoeckenius, W. *Methods Enzymol.* **1974**, *31*, 667–678.
(73) Hamm, P.; Zurek, M.; Röschinger, R.; Patzelt, H.; Oesterhelt, D.; Zinth, W. *Chem. Phys. Lett.* **1997**, *268*, 180–186.
(74) Smith, S. O.; Myers, A. B.; Mathies, R. A.; Pardoen, J. A.; Winkel, C.; van den Berg, E. M. M.; Lugtenburg, J. *Biophys. J.* **1985**, *47*, 653–664.
(75) Smith, S. O.; Braiman, M. S.; Myers, A. B.; Pardoen, J. A.; Courtin, J. M. L.; Winkel, C.; Lugtenburg, J.; Mathies, R. A. *J. Am. Chem. Soc.* **1987**, *109*, 3108–3125.
(76) Edler, J.; Hamm, P. *J. Chem. Phys.* **2002**, *117*, 2415–2424 (Appendix B).
(77) Uhmann, W.; Becker, A.; Taran, C.; Siebert, F. *Appl. Spectrosc.* **1991**, *45*, 390–397.
(78) Terentis, A. C.; Ujj, L.; Abramczyk, H.; Atkinson, G. H. *Chem. Phys.* **2005**, *313*, 51–62.
(79) Lohrmann, R.; Stockburger, M. *J. Raman Spectrosc.* **1992**, *23*, 575–583.
(80) Brack, T. L.; Atkinson, G. H. *J. Phys. Chem.* **1991**, *95*, 2351–2356.
(81) Ye, T.; Friedman, N.; Gat, Y.; Atkinson, G. H.; Sheves, M.; Ottolenghi, M.; Ruhman, S. *J. Phys. Chem. B* **1999**, *103*, 5122–5130.
(82) Hasson, K. C.; Gai, F.; Afinrud, P. A. *Proc. Natl. Acad. Sci. U.S.A.* **1996**, *93*, 15124–15129.
(83) Rödig, C.; Chizhov, I.; Weidlich, O.; Siebert, F. *Biophys. J.* **1999**, *76*, 2687–2701.

JP810397U